LBNL-51488

Submitted to the

Journal of Applied Physics

Ion energy distribution functions of vacuum arc plasmas

Eungsun Byon and André Anders

Lawrence Berkeley National Laboratory, University of California,
1 Cyclotron Road, MS 53, Berkeley, California 94720-8223

September 13, 2002

Corresponding Author:
André Anders
Lawrence Berkeley National Laboratory
1 Cyclotron Road
Berkeley, CA 94720-8223, USA
Tel. + (510) 486-6745
Fax + (510) 486-4374
e-mail aanders@lbl.gov

This work was supported by the U.S. Department of Energy, under Contract No. DE-AC03-76SF00098, Eungsun Byon was supported by the post-doctoral fellowship program of the Korean Science and Engineering Foundation (KOSEF)

Ion energy distribution functions of vacuum arc plasmas

Eungsun Byon and André Anders[a]

Lawrence Berkeley National Laboratory, University of California,

1 Cyclotron Road, MS 53, Berkeley, California 94720-8223

Abstract

The velocity distribution function of vacuum arc ions can be measured by a time-of-flight technique similar to a method originally proposed by Yushkov. The measuring principle makes use of the well-justified assumption that the ion drift velocity from the cathode spot region to a collector is approximately constant. It is shown that the negative time derivative of the collector current is directly proportional to the ion distribution function provided that the time-averaged source intensity (i.e., emission of ions from cathode spots) is constant until the arc is rapidly switched off. In the experiment, arc termination took about 700 ns, which is much faster than the decay of the ion current measured at the collector placed in more than 2 meters distance from the cathode. The experimental distribution functions for most cathode materials show one large peak with a tail and one or more small peaks at higher ion velocities. The distribution functions for some other materials exhibit several peaks. No conclusive answer can be given about the nature of these peaks. Arguments are presented that the peaks are not caused by different charge states or plasma contamination but rather due to insufficiently averaged source fluctuations and/or acceleration by plasma instabilties.

[a] Author to whom correspondence should be addressed; electronic mail: aanders@lbl.gov

I. INTRODUCTION

There are numerous studies of kinetic ion energies of vacuum arc plasmas[1-7] because these energies are surprisingly high (up to 200 eV) and of great technological relevance for synthesis of dense coatings. Most studies deal with the determination of *average* velocities, which can readily be converted into average ion energies according to

$$\overline{E_{kin}} = \frac{m_i}{2}\left(\overline{v_i}\right)^2 \tag{1}$$

However, very few studies have been done to determine velocity or kinetic ion energy *distribution functions*, as opposed to the average or most likely velocity or kinetic energy. Ideally, one would measure the energy distribution function for each particle species present in the plasma. This has been done by Plyutto et al.[2], Davis and Miller[3], and Yushkov[8]. The measurements are difficult and require sophisticated equipment and data analysis procedure. For example, Yushkov[8] could show that all charge states of a vacuum arc for a given cathode material have approximately the same velocity. However, some uncertainty remained due the sensitivity of the ion extraction optics on the plasma density. In this work, the focus is on the careful determination of charge-state-integrated ion distribution functions. No ion extraction system is used, and thus all distortions by ion optics are eliminated. The price for energy resolution in the distribution function is the loss of species sensitivity compared to Yushkov's experiment[8]. The resolution of the present experiment is significantly improved compared to previous experiments by means of increasing the plasma drift length to more than 2 meters, and by collecting and processing the data through modern, fast data acquisition systems. Additionally, energy distribution functions are presented for the first time for a number of cathode materials.

II. THEORY

The idea to measure the energy distribution function is based on measurements of the time ions need to drift from the source, the cathode spot, to an ion detector at a well-known distance d. It is assumed that ion acceleration occurs mainly in the vicinity of the cathode spot, where the pressure and field gradients are very high, and the ion velocity is approximately constant for the rest of the drift from the discharge region to the ion collector. This assumption is justified through previous experiments and

theories (e.g. Ref.[9-14]), which indicate an acceleration zone of less than 1 mm. The assumption will be checked and discussed in section IV of this work. With this assumption, the time of flight is simply

$$t = d/v\,. \tag{2}$$

In order to derive the correct expression linking the velocity distribution with the observable detector current, one can start by considering an infinitesimally short emission of ions having a velocity distribution $f(v)$. The detector would record a current signal $i(t)$ of finite duration, which directly reflects the velocity distribution, i.e.,

$$f(v) = C\, i(t) \tag{3}$$

where C is a constant. The cathode spot emits particles in a very rapid sequence of bursts, and thus one can assume that source bursts would cause a signal at the detector that can be written as

$$I(t) = \int_0^t \sigma(t')\, i(t'-t)\, dt' \tag{4}$$

where $\sigma(t)$ is the time dependent source intensity. In the following it will be shown that the derivative of the ion collector current, dI/dt, contains information on the velocity distribution. This can easily be done using the Laplace transformation

$$\Lambda\big(y(t)\big) \equiv \int_0^\infty \exp(-st)\, y(t)\, dt \tag{5}$$

where $y(t)$ is a complex function of the real variable t. Applying the Laplace transformation to the time derivative of Eq.(4) gives

$$\begin{aligned} \Lambda\left(\frac{dI}{dt}\right) &= \Lambda\left(\frac{d}{dt}\int_0^t \sigma(t')\, i(t'-t)\, dt'\right) \\ &= s\,\Lambda\left(\int_0^t \sigma(t')\, i(t'-t)\, dt'\right) \\ &= s\,\Lambda\big(\sigma(t)\big)\,\Lambda\big(i(t)\big) \end{aligned} \tag{6}$$

where s is the variable in Laplace space. In the simplest case, the source function is a step function which is constant before, and zero after the source is switched off at time t_1, i.e.,

$$\sigma(t) = A\,\theta(t) \quad \text{and} \quad \theta(t) \equiv \begin{cases} 1 & \text{for } 0 < t < t_1 \\ 0 & \text{for } t > t_1 \end{cases} \tag{7}$$

where A is the amplitude. Using

$$\Lambda\left(\theta\left(t\right)\right)=\frac{1-\exp\left(-t_1 s\right)}{s} \tag{8}$$

as the Laplace-transformed step function, one obtains from Eqs. (6) and (7)

$$\Lambda\left(\frac{dI}{dt}\right)=A\left[\Lambda\left(i\left(t\right)\right)-\exp\left(-t_1 s\right)\Lambda\left(i\left(t\right)\right)\right] \tag{9}$$

and, by inverse Laplace transformation,

$$\frac{dI}{dt}=A\left[i\left(t\right)-i\left(t-t_1\right)\right]. \tag{10}$$

The first term in the RHS bracket is the contribution from turning on the source at time zero, and the second term results from switching it off at the time t_1. Obviously, the time of constant emission from the source does not contribute to the time derivative in Eq.(10). If turning on of the source occurred a long time ago, only switching off the source will contribute to dI/dt. Mathematically, if turning off of source occurred at t_1 and

$$t_1 >> t_0 = d/v_{\min}\,, \tag{11}$$

where $v_{\min} > 0$ is the smallest velocity in the distribution function, than Eq.(10) can be simplified to

$$\frac{dI\left(t\right)}{dt}=-A\,i\left(t-t_1\right). \tag{12}$$

and with Eq.(3), the final result is

$$f\left(v\right)=-c\frac{dI\left(t+t_1\right)}{dt} \tag{13}$$

where the new factor *c* is composed of the previously introduced constants, $c = C/A$. This simple relation is the basis for the measurements presented in section III.

It is interesting to consider a physically more realistic, slower switch-off of the source, e.g.,

$$\sigma\left(t\right)=\begin{cases} 1 & \text{for } 0<t<t_1 \\ \exp\left(-\dfrac{t-t_1}{\tau}\right) & \text{for } t>t_1 \end{cases} \tag{14}$$

instead of the step function (7); the amplitude *A* was set to unity for simplicity, and τ is the characteristic decay time of the source. One would use the Laplace transformations

$$\Lambda(1)=\frac{1}{s} \quad \text{and} \quad \Lambda\left(1-\exp\left(-\frac{t-t_1}{\tau}\right)\right)=\frac{\exp(-t_1 s)}{s(\tau s+1)} \tag{15}$$

to get

$$\Lambda(\sigma(t))=\frac{1}{s}-\frac{\exp(-t_1 s)}{s(\tau s+1)} \ . \tag{16}$$

Plugging this in Eq.(6) gives

$$\Lambda\left(\frac{dI}{dt}\right)=\left(1-\frac{\exp(t_1 s)}{\tau s+1}\right)\Lambda(i(t)) \ . \tag{17}$$

Inverse Laplace transformation results in

$$\frac{dI}{dt}=i(t)-\int_{t_1}^{t}\frac{1}{\tau}\exp\left(-\frac{t'-t_1}{\tau}\right)i(t-t')dt' \tag{18}$$

in analogy to Eq.(10). Also here, the first term of the RHS is due to switching on the source, and the second term is due to the slow switching off. This expression however cannot be brought to a simple analytical form for the velocity distribution, and evaluation of data needs to be done numerically. For $\tau \to 0$ the integral converges to the previous result (10) describing a source that was instantaneously switched off. Thus is it desirable to work with a very short switch-off time in order to utilize the simplest relationship (13) for data evaluation. The condition to the experiment can be expressed as

$$\tau=\left|\frac{1}{I_{arc}}\frac{dI_{arc}}{dt}\right|^{-1} << \left|\frac{1}{I}\frac{dI}{dt}\right|^{-1} . \tag{19}$$

where I_{arc} is the arc current and *I* is the ion current at the collector. This condition can be fulfilled by (i) rapidly switching off the arc, and (ii) reducing the fall rate of the ion current by using a long drift path.

III. EXPERIMENTAL

The experiments were performed in the vacuum chamber of Berkeley's vacuum arc ion source "Mevva V." In contrast to usual operation[15], the ion extraction system was removed to use the entire length of the system for plasma drift without ion beam formation. The cathode plasma was generated at cathode spots on the front face of a cylindrical cathode of 6.25 mm diameter. The annular anode had an inner diameter of 13 mm; the closest cathode-to-anode distance was about 5 mm. The cathode was mounted on a carrousel holding a total of 18 cathodes, and therefore a number of cathode materials could be used without

interrupting vacuum. The vacuum chamber was cryogenically pumped to a base pressure of about 4 x 10^{-5} Pa.

The arc discharge was fed by an 8-stage pulse-forming-network (PFN) of 1 Ω impedance delivering a nearly rectangular arc pulse shape of 250 μs duration and 100-500 A amplitude depending on the charging voltage. The arc pulse repetition rate was 1 p.p.s. unless indicated otherwise. The plasma expanded from the cathode spot region into the main vacuum vessel, and part of the plasma kept drifting though a tube that is usually part of the time-of-flight charge-to-mass spectrometer[16]. At the end of the tube, a metal plate of 100 cm^2 area is used as an ion collector. The plate was negatively biased to –70 V, i.e. it is operating in the ion saturation regime. Secondary electrons can be neglected at the relatively low energy of ions impacting the collector. The distance from the cathode surface to the ion collector was d = 2.153 m.

The arc discharge could be rapidly terminated by re-routing the arc current into a short circuit of lower impedance than the arc circuit using a high-current thyristor. This technique has been demonstrated previously[7,8]. The schematic is shown in Figure 1. When the thyristor is triggered and becomes conducting, the arc discharges current between cathode and anode ceases with a fall time of about 700 ns, as measured by a wide-band Pearson current transformer, model 301X. The finite fall time is due to the inductance of the thyristor circuit and the intrinsic switching time of the high-current thyristor, which was specified as 500 ns by the manufacturer.

The rapid fall of the arc current is used to trigger a 500 MHz digital storage oscilloscope (Tektronix TDS 744), giving the "zero" time mark for the data stored in the scope's memory. The ion saturation current of the ion collector shows a very distinct delay due to the time-of-flight from the cathode spot upon arrival at the collector. The falling curve contains information on the ion distribution function as shown in section II. Since plasma production is noisy, and fluctuations of the intensity of production cannot by distinguished from a variation in the velocity distribution. A large number of measurements needs to be averaged to eliminate the effects of plasma noise. That means, mathematically, that averaging is used to make the source function $\sigma(t)$ constant before switch-off. We used 100 arc discharges to obtain one average ion current function $I(t)$ for a given cathode material at constant discharge conditions. Each data

curve $I(t)$ contained 50,000 data points, allowing us to utilize these curves for numerical smoothing and differentiation. Figure 2 shows an example of measured averaged arc and ion currents.

IV. RESULTS AND DISCUSSION

The ion current curves $I(t)$ have been used to derive the ion distribution functions using the simple relation (13). Figures 3-5 show typical results for a number of cathode materials. As one can see, most distribution functions tend to consist of one large, relatively narrow peak plus a tail at higher velocities which may have one or several smaller peaks. There are also a few distributions that exhibit an asymmetric shape, characterized by a several peaks and a broader tail at higher energies.

One might be tempted to suggest that tail and peaks could be caused by higher charge states or contamination of lower mass such as oxygen or hydrogen. Unfortunately, no conclusive answer can be derived from the present data due to the lack of species resolution. However, one can make a few statements based on the present data and on independent findings described in the literature.

First, using basically the same time-of-flight technique but with ion extraction, Yushkov[8] showed that the ion velocity distributions are approximately independent of the ion charge state. His pioneering experiments would have put the issue to rest if the results were free of aberration in the ion optics. Density modulations, either as periodic oscillations or sharp cut-off as utilized here, cause deformation of the plasma-sheath meniscus at the ion extraction grid, a problem known as the perveance matching issue[17]. As a result, the beam of extracted ions carries convoluted information on ion density in the plasma and shape of the meniscus. This shortcoming was the main reason why we did not use an ion extraction system for the present investigation. One may suppose that aberrations caused some systematic deviations but did not alter the result entirely. That would be an argument that the local peaks seen at the high-velocity tail are not caused by higher charge states.

Second, large the peak in the *velocity* distribution usually appears at low velocities, even in cases when the ion *charge state* distribution[18] is known to have a maximum for charge state greater than one. For example, aluminum has 38% single charge, 51% double charge, and 11% double charge ions in the plasma. If the ion velocity or kinetic energy was directly associated with acceleration in an electric field (like in the potential hump hypothesis[2,3]), the velocity distribution function should show one peak for each charge state.

In the example of aluminum, if we assumed that the second peak of the velocity distribution function corresponds to charge state 2+, this peak should be highest. This is not the case: the first peak at low velocity is the highest. This disagreement appears even stronger keeping in mind that electrical currents, rather than particles currents, are used to display the distribution function. Therefore, the ion charge state acts like a weight factor in the distributions displayed. Doubly charged ions contribute twice the signal compared to singly charged ions.

Third, we can also exclude that contamination by species of lighter mass cause peaks at the high-velocity tail. This statement can be made because the amount of lighter ions such as oxygen and hydrogen is very small (a few percent or less), with the exception of the beginning of an arc pulse[19]. The forced current-zero of the arc discharge was done about 200 μs after arc triggering, and therefore the amount of contamination should be very small at that time. Yet another argument can be brought by investigating the dependence of the high-velocity tail on the pulse repetition rate. It is known that the level of contamination decreases dramatically with increasing arc pulse repetition rate or arc duty cycle[20]. Therefore, the high-velocity tail should disappear at high pulse repetition rate if it was caused by light-mass contamination. Figure 6 shows that this is not the case.

Fourth, one may wonder how sensitively the data depend on the arc current. It is known that plasma production occurs are cathode spots, and that higher current causes the number of arc spots to increase rather than to change the character of the spot itself[21]. Based on this knowledge one would expect that the arc current has only a small effect on the measured distributions. This is indeed the case, as illustrated by Fig. 7, at least for the current range investigated. Though, there may be noticeable changes if the arc current was very small, i.e. near the arc chopping current, or at very high currents, when the plasma streams from many arc spots start interacting, and also when magnetic fields were present. These cases have not been studied here.

The present result can be compared with previous measurements[2,3,7,8,22] of distribution functions and average energies. Since the distribution functions are not quite symmetric, one has to be careful about referring to the most likely versus the average velocity: the high-velocity tail and its local peaks cause the average velocity to be higher than the most-likely velocity. On the other hand, most distribution functions exhibit a large, nearly symmetric peak, dominating the distribution, and using the peak values is a good

characteristic figure of merit to be compared with literature data of velocities. Figure 8 shows a comparison of most likely velocities measured here with literature data of ion velocities. Generally, there is very good agreement. A characteristic pattern can be confirmed that has been associated with materials properties as grouped in the Periodic Table of elements. As pointed out in previous work[7], these properties are reflected in the material-dependent electron temperature, which gives, in the model of adiabatic plasma expansion, a simple expression for the ion velocity[23]:

$$v_i \approx 3.5\sqrt{Q\gamma kT_e^* / m_i} \tag{20}$$

where T_e^* denotes the electron temperature at the point where ions become supersonic, $\overline{Q}$ is the average ion charge state, and $\gamma \approx 5/3$ is the adiabatic coefficient.

The fact that the present measurements agree well with literature data is a strong argument for the assumption that most of the ion acceleration occurred in the vicinity of cathode spot, while the velocity is approximately constant when the plasma streams towards the detector. In our case, the drift length was over two meters while in most other experiments it was less than 0.3 meters.

Because no species resolution was done here, work still remains to be done to clarify the composition and ultimately the cause of the peaks seen in some of the distributions. At least in part, such peaks could be due to the explosive nature of plasma production, making the averaged source function not constant, $\overline{\sigma(t)} \neq const.$ for $0 < t < t_1$, i.e. violating an assumption made for the evaluation of data. Another reason could be ion acceleration by plasma instabilities. For example, Ivanov and co-workers[24] argued that the Buneman instability can cause ion acceleration. Krinberg and co-workers[25] used a magneto-hydrodynamic model and pointed out that local pinching by a magnetic field can lead to ion acceleration and jet formation, especially while the discharge current is rising. This has been shown to be true in the vacuum spark regime when the discharge current has a rise rate exceeding 3×10^8 A/s : ion kinetic energies up to 10 keV have been observed[26-28]. It is generally accepted that electron-ion coupling in the expanding plasma[9-13] plays a crucial role for ion acceleration, and ion acceleration due to electrostatic fields does not explain the present or other literature data. Obviously, there is a wealth of phenomena. To give theoreticians a good foundation, future work should address the nature of various peaks seen in the

distribution function by discriminating between different ion charge states while maintaining high energy resolution.

ACKNOWLEDGEMENTS

We gratefully acknowledge helpful discussion with Jörg Zimmermann and George Yushkov as well as technical assistance by Robert MacGill. This work was supported by the U.S. Department of Energy under Contract No. DE-AC03-76SF00098. Eungsun Byon was supported by the post-doctoral fellowship program of the Korean Science and Engineering Foundation (KOSEF).

FIGURE CAPTIONS

FIG. 1. Schematic of the experimental setup.

FIG. 2. Example of arc and ion currents, averaged over 100 individual discharges.

FIG. 3. Ion velocity distributions for C, Mn, Ti, V, Sb, Mg, Cr, and Ge.

FIG. 4. Ion velocity distributions for Sc, Al, Ag, Sm, Y, In, Co, and Er.

FIG. 5. Ion velocity distributions for Ni, Zr, Cu, Mo.

FIG. 6. Ion velocity distributions for various cathode materials, measured at four different arc pulse repetition rates.

FIG. 7. Ion velocity distributions for various arc currents; no significant change can be found in the current range investigated.

REFERENCES

[1] R. Tanberg, Phys. Rev. **35,** 1080-1089 (1930).

[2] A. A. Plyutto, V. N. Ryzhkov, and A. T. Kapin, Sov. Phys. JETP **20,** 328-337 (1965).

[3] W. D. Davis and H. C. Miller, J. Appl. Phys. **40,** 2212-2221 (1969).

[4] A. S. Bugaev, V. I. Gushenets, A. G. Nikolaev, E. M. Oks, and G. Y. Yushkov, IEEE Trans. Plasma Sci. **27,** 882-887 (1999).

[5] A. S. Bugaev, E. M. Oks, G. Y. Yushkov, A. Anders, and I. G. Brown, Rev. Sci. Instrum. **71,** 701-703 (2000).

[6] G. Y. Yushkov, A. Anders, E. M. Oks, and I. G. Brown, J. Appl. Phys. **88,** 5618-5622 (2000).

[7] A. Anders and G. Y. Yushkov, J. Appl. Phys. **91,** 4824-4832 (2002).

[8] G. Yushkov, in *IXX Int. Symp. on Discharges and Electrical Insulation in Vacuum* (Xi'an, P.R. China, 2000), p. 260-263.

[9] C. Wieckert, Contrib. Plasma Phys. **27,** 309-330 (1987).

[10] C. Wieckert, Phys. Fluids **30,** 1810-1813 (1987).

[11] E. Hantzsche, J. Phys. D: Appl. Phys. **24,** 1339-1353 (1991).

[12] E. Hantzsche, IEEE Trans. Plasma Sci. **34,** 34-41 (1992).

[13] E. Hantzsche, IEEE Trans. Plasma Sci. **23,** 893-898 (1995).

[14] S. Anders and A. Anders, J. Phys. D: Appl. Phys. **21,** 213-215 (1988).

[15] I. G. Brown, Rev. Sci. Instrum. **65,** 3061-3081 (1994).

[16] I. G. Brown, J. E. Galvin, R. A. MacGill, and R. T. Wright, Rev. Sci. Instrum **58,** 1589-1592 (1987).

[17] A. T. Forrester, *Large Ion Beams* (Wiley, New York, 1988).

[18] A. Anders, Phys. Rev. E **55,** 969-981 (1997).

[19] J. M. Schneider, A. Anders, B. Hjörvarsson, and L. Hultman, Appl. Phys. Lett. **76,** 1531-1533 (2000).

[20] G. Y. Yushkov and A. Anders, IEEE Trans. Plasma Sci. **26,** 220-226 (1998).

[21] B. Jüttner, J. Phys. D: Appl. Phys. **34,** R103-R123 (2001).

[22] J. Kutzner and H. C. Miller, J. Phys. D: Appl. Phys. **25,** 686-693 (1992).

[23] I. A. Krinberg, Techn. Phys. **46,** 1371-1378 (2001).

[24] V. A. Ivanov, S. Anders, B. Jüttner, and H. Pursch, in *XIVth Int. Symp. Discharges and Electrical Insulation in Vacuum*, edited by R. W. Stinnett (Sandia, Santa Fe, NM, 1990), p. 192-197.

[25] I. A. Krinberg and V. L. Paperny, J. Phys. D: Appl. Phys. **35,** 549-562 (2002).

[26] A. A. Plyutto, Z. Exp. Theor. Fiz. (USSR) **39,** 1589-1592; Engl. Transl: Sov. Phys J. Exp. Theor. Phys. **12** (1961) 1106-1108 (1960).

[27] N. V. Astrakhanstsev, V. I. Krasov, and V. L. Paperny, J Phys. D: Appl. Phys. **28,** 2514-2518 (1995).

[28] S. P. Gorbunov, V. I. Krasov, and V. L. Paperny, J. Phys. D: Appl. Phys. **30,** 1922-1927 (1997).

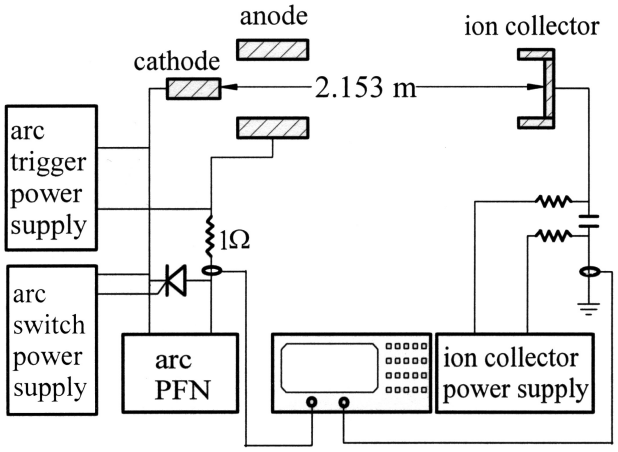
anode
ion collector
cathode
2.153 m
arc
trigger
power
supply
1Ω
arc
switch
power
supply
arc
PFN
ion collector
power supply

Figure 1

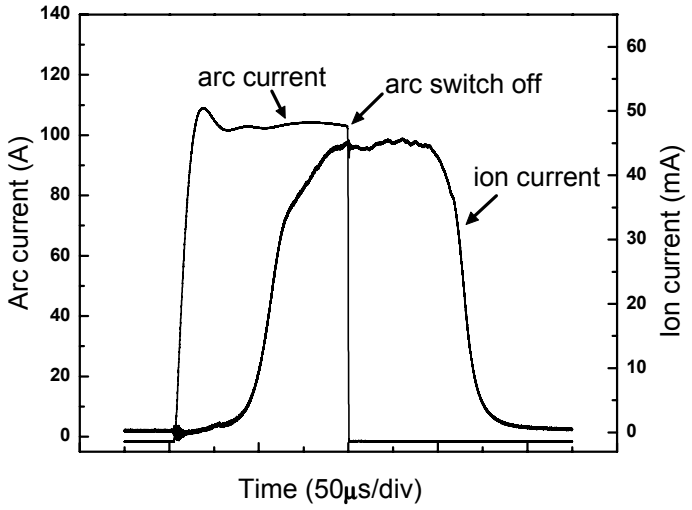
arc current
arc switch off
ion current
Arc current (A)
Ion current (mA)
Time (50μs/div)
140
120
100
80
60
40
20
0
60
50
40
30
20
10
0

Figure 2

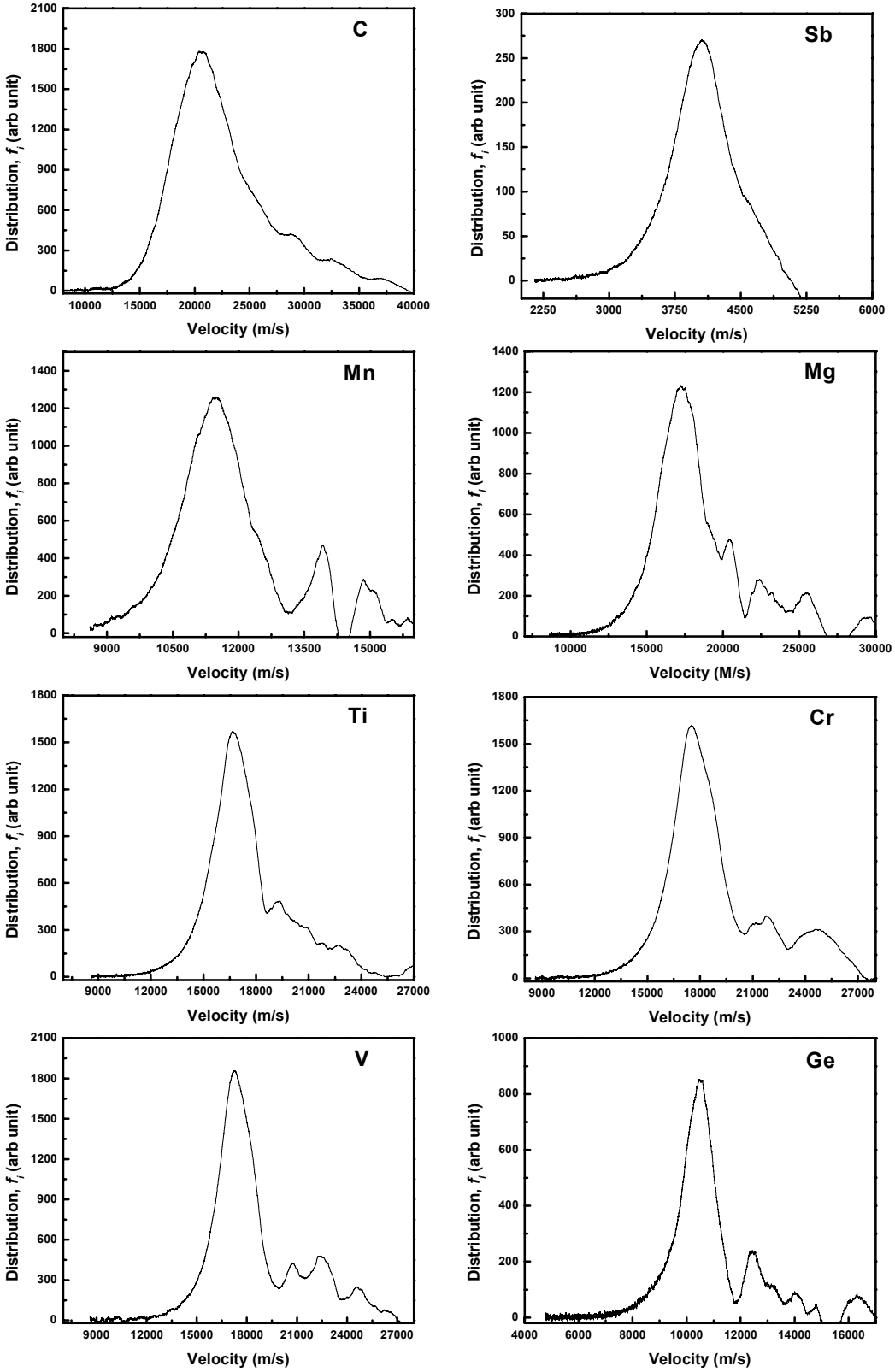
C
Distribution, f_i (arb unit)
Velocity (m/s)
Sb
Distribution, f_i (arb unit)
Velocity (m/s)
Mn
Distribution, f_i (arb unit)
Velocity (m/s)
Mg
Distribution, f_i (arb unit)
Velocity (M/s)
Ti
Distribution, f_i (arb unit)
Velocity (m/s)
Cr
Distribution, f_i (arb unit)
Velocity (m/s)
V
Distribution, f_i (arb unit)
Velocity (m/s)
Ge
Distribution, f_i (arb unit)
Velocity (m/s)

Figure 3

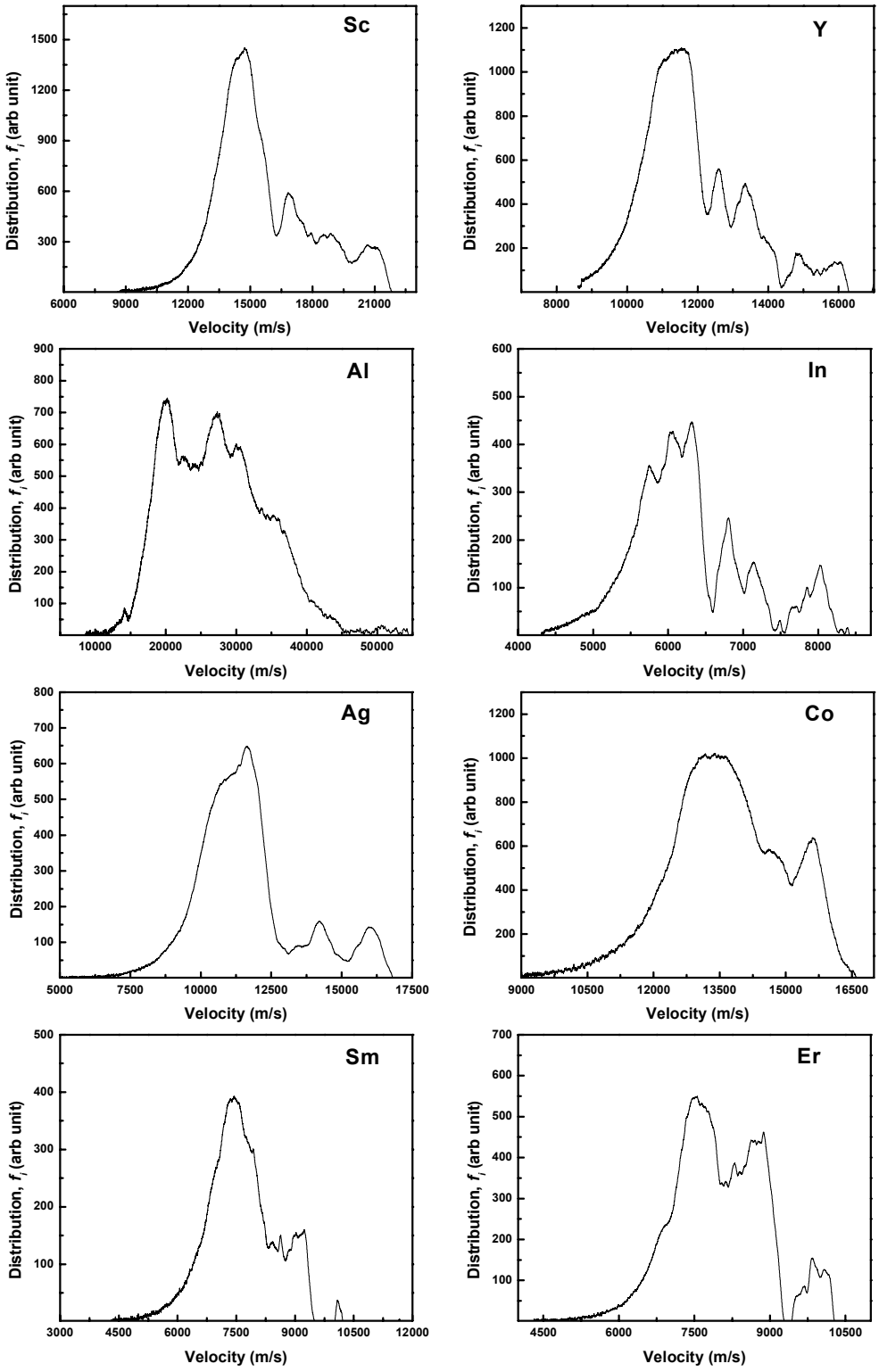

Figure 4

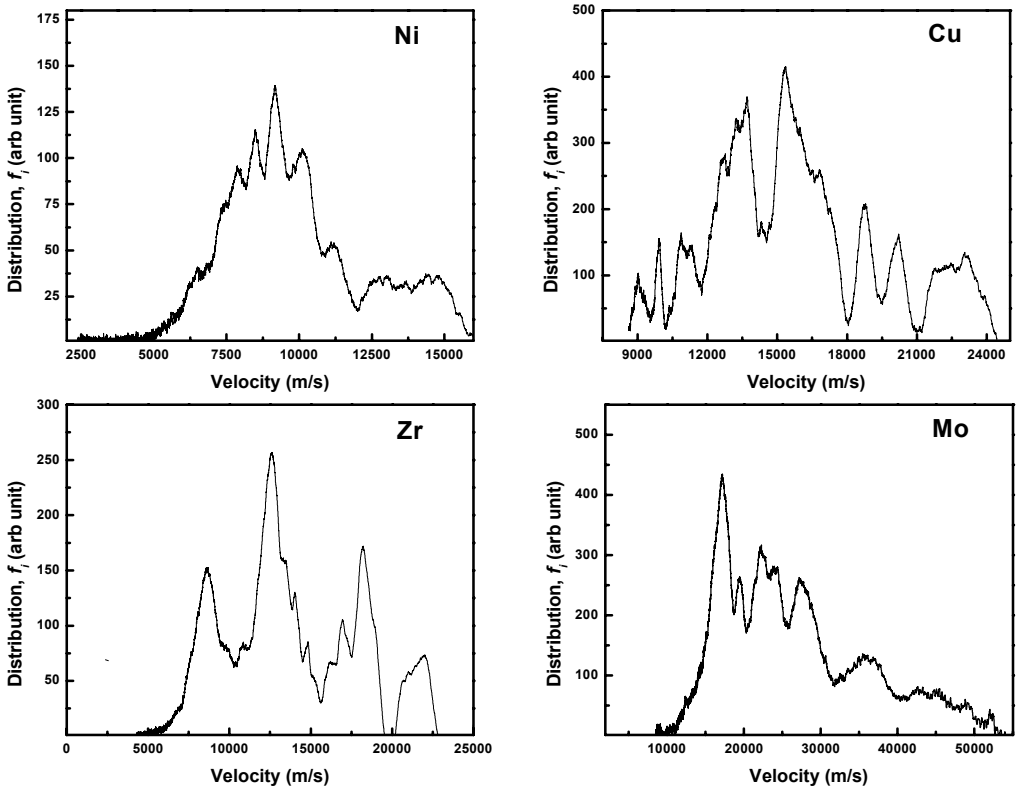

Figure 5

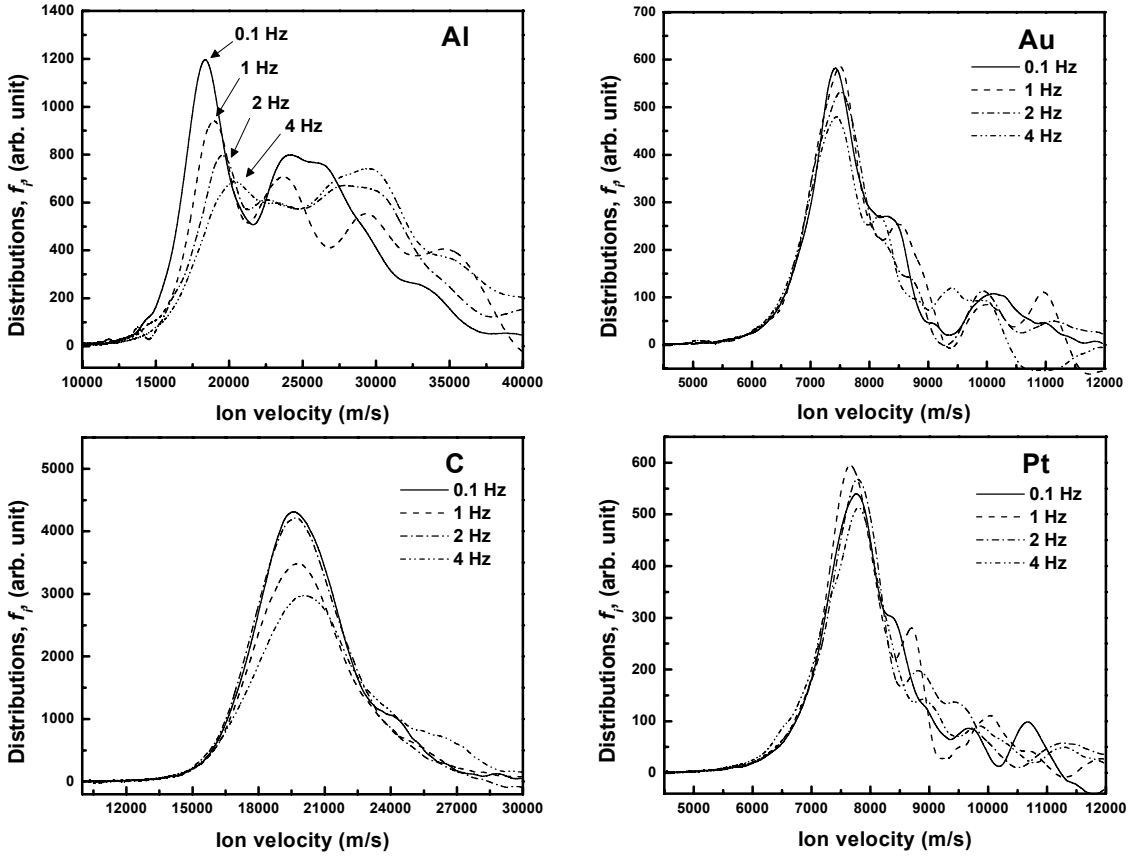
Al
0.1 Hz
1 Hz
2 Hz
4 Hz
Distributions, f_p (arb. unit)
Ion velocity (m/s)
Au
0.1 Hz
1 Hz
2 Hz
4 Hz
Distributions, f_p (arb. unit)
Ion velocity (m/s)
C
0.1 Hz
1 Hz
2 Hz
4 Hz
Distributions, f_p (arb. unit)
Ion velocity (m/s)
Pt
0.1 Hz
1 Hz
2 Hz
4 Hz
Distributions, f_p (arb. unit)
Ion velocity (m/s)

Figure 6

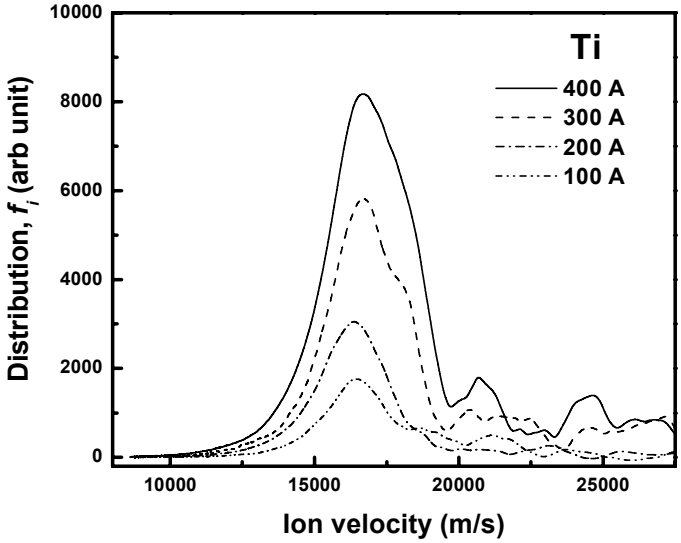
Ti
400 A
300 A
200 A
100 A
Distribution, f_i (arb unit)
Ion velocity (m/s)
10000
8000
6000
4000
2000
0
10000
15000
20000
25000

Figure 7

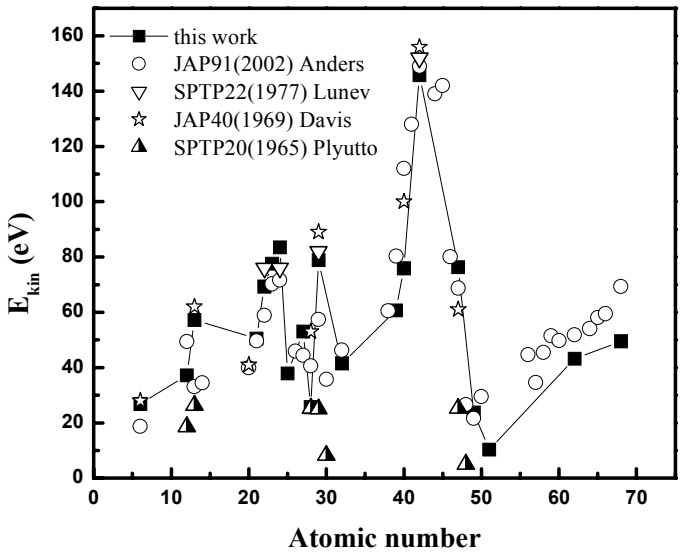
this work
JAP91(2002) Anders
SPTP22(1977) Lunev
JAP40(1969) Davis
SPTP20(1965) Plyutto
E_{kin} (eV)
Atomic number
0
20
40
60
80
100
120
140
160
0
10
20
30
40
50
60
70

Figure 8